E-proceedings of the 38th IAHR World Congress
September 1-6, 2019, Panama City, Panama
doi:10.3850/38WC092019-1581

CATCHING THE VEGETATION DYNAMICS AT THE REACH SCALE USING SATELLITE IMAGERY

MICHAEL NONES(1), MASSIMO GUERRERO(2)

(1) Department of Hydrology and Hydrodynamics, Institute of Geophysics, Polish Academy of Science, Warsaw, Poland, mnones@igf.edu.pl

(2) Department of Civil, Chemical, Environmental, and Materials Engineering, University of Bologna, Italy, massimo.guerrero@unibo.it

ABSTRACT

The cloud-based platform Google Earth Engine was used to evaluate the changes of the Normalized Difference Vegetation Index (NDVI) on a lowland reach of the Po River, Italy. Using the 30m resolution Landsat8 images, the study covered the April-October growing season in the 2013-2017 period and considered three different zones: a curve, a central bar and an island. Observing the variations of the NDVI across the areas it is possible to retrieve qualitative information about the vegetation encroachment and the correlated changes of the local river morphology. In the case of the curve, the inner bank was subjected to deposition and the vegetation improved this trend, stabilizing the bar and moving the current towards the outer bank, more stable. As for the central bar, the plants' encroachment contributed to increasing the dimension of the bar, providing additional room for future plants and changing the bar morphology towards a stable island. In the third case, the island was already formed, and the NDVI remained almost constant during the observed period, indicating that plants have already stably colonized this area. The NDVI was correlated to the water discharges measured upstream of the study sites, pointing out a slight dependence of the riparian vegetation growth from the water flow and on the seasons. However, such a correlation is not yet well explained because of the short temporal horizon here evaluated.

This paper represents a first attempt to use the free service Google Earth Engine to characterize the medium-term behaviour of riparian vegetation establishment on different fluvial landscapes, improving our knowledge about the reciprocal feedback between hydrology, fluvial morphology and plant dynamics at the reach scale.

Keywords: Google Earth Engine; NDVI; Po River; river dynamics; vegetation growth

1 INTRODUCTION

Nowadays, the human pressure on alluvial rivers is constantly increasing, affecting all the components at different time scales. The effects of transient hydrology, driven by climatic or anthropogenic conditions, on the riparian vegetation and the bed morphology are not immediate, and therefore a longer and large-scale record should be considered to catch them properly. To correctly model the water-sediment-vegetation interactions in fluvial environments it is necessary, therefore, to adopt adequate monitoring techniques like satellite imagery, which cover a longer period with a good resolution and can be easily handled for specific purposes.

The use of satellite imagery for evaluating changes of different environmental parameters at manifold spatiotemporal scales is becoming very popular in recent years, being correlated with the improvement of computational tools. Many commercial and freeware services are rising for handling satellite information, providing scientists and practitioners with the opportunity to study the dynamics of the natural and anthropic environment also in areas otherwise hardly difficult to reach (e.g., Bizzi et al., 2016; Bechter et al., 2018; Monegaglia et al., 2018).

Among others, the freeware service Google Earth Engine (GEE) is in use across a wide variety of disciplines, covering topics like vegetation establishment (Hansen et al., 2013; Tsai et al., 2018) water surface (Pekel et al., 2016) and sediment field (Markert et al., 2018) dynamics, crop yield estimation (Lobell et al., 2015; Shelestov et al., 2017), land cover (Carrasco et al., 2019) and rice paddy mapping (Dong et al., 2016), urban (Patel et al., 2015; Zhang et al., 2015) and flood mapping (Coltin et al., 2016), fire recovery (Soulard et al., 2016), as well as health risk mapping (Sturrock et al., 2014). Several applications to riverine environments (e.g., Edmonds et al., 2016; Isikdogan et al., 2017) proved the reliability of this tool in evaluating the medium- to long-term dynamics acting at the reach scale.

The contemporary long-time satellite remote sensing data provides an advanced way to monitor the surface vegetation dynamics in relation to climate and environmental variations at different spatiotemporal scales (Yang et al., 2013; Huete, 2016). Since the earliest work in the 1970s (Tucker et al., 1973; Rouse, 1974), the

Normalized Difference Vegetation Index (NDVI) is one of the most widely implemented remote sensing spectral index for monitoring Earth's land surface (Robinson et al., 2017; Chu et al., 2019). The index capitalizes on the optical properties of the cellular structure of leaves: the photosynthetic pigments absorb radiation in the visible range of the spectrum and reflect radiation in the near-infrared (NIR) range. The simple formula of NDVI and its direct relationship to vegetation photosynthetic capacity is a proxy for a wide range of essential vegetation characteristics and functions (e.g., a fraction of photosynthetic radiation absorbed by the canopy, leaf area, canopy "greenness", etc.) with countless applications in all the vegetation-related sciences.

The Italian Po River represents a perfect example of the impact that human pressure can have on fluvial environments. Starting from the late '800 the river was straightened by levees, which frozen the planform configuration, while the extensive longitudinal bank protection works have altered the lateral sediment exchange sediments, with the consequent reduction and closure of many secondary channels (Lanzoni et al., 2015). The incision of the active bed has been further enhanced by the construction of dams and groynes (Maselli et al., 2018), as well as by a massive sediment excavation activity in the period 1960-1990 (Lamberti and Schippa, 1994). The morphological consequences of all these human interventions were initially quite fast and led to a significant and generalized deepening of the middle reach of the river in the period 1954–1980 (Castiglioni et al., 1999; Marchetti, 2002; Guerrero et al, 2013). Nowadays, the Po River is a relatively straight channel, having lost its meandering pattern especially in its intermediate and low reaches but, in the last decades, the anthropogenic pressure on the river decreased producing morphological quasi-equilibrium conditions, where eroded and deposited volumes tend to compensate each other (Lanzoni et al., 2015).

Aside from geomorphic analyses, the impact of humans on ecosystem services is addressed worldwide with different techniques (de Jalón et al., 2017), but the influence of plants on river channel topography and the feedback effects are still poorly understood, in particular for a variable sediment supply (Diehl et al., 2017). Several experimental (Fergus, 1997; Choi et al., 2005; Bollati et al., 2014) and numerical (Nones et al., 2013; Eke et al., 2014) studies shown that a reduction of variability in water and sediment discharges fosters the encroachment of the vegetation over exposed bars and along the banks. The increase of vegetation cover definitely contributes to stabilizing the sediments and in further reducing the river wandering. However, reliable estimates at the reach scale and covering long periods are still lacking because of the difficulties in obtaining significant datasets.

After the description of the study site, the main tools used in the analysis are briefly presented. On the one side, the preliminary results reported here provide some insights on the reciprocal feedback between the fluvial hydro-morphology and the riparian vegetation. On the other side, they pointed out the need for performing long-term studies at the reach scale for having more reliable estimates, because of the scale involved. Aside from the present outcomes, also the future steps will be discussed in the paper, aiming to provide a general overview of using remote sensing imagery for evaluating the Po River dynamics during the more recent years.

2 CASE STUDY

The Po River is the longest watercourse in Italy, flowing eastward across northern Italy for around 660 km (Figure 1a) and draining a considerably rich and diversified in geographical, demographic and socio-economic terms, but generally highly anthropized basin of about 74,700 km² (Domeneghetti et al., 2015; Musolino et al., 2017). The long-term time series measured at the gauging station of Piacenza shows that the annual hydrograph has two peaks in discharge in autumn and spring, generated by rainfall and snowmelt, respectively (Zanchettin et al., 2008; Montanari, 2012). The long-term mean annual discharge at the Borgoforte (Mn) gauging station is around 1000–1300 m^3/s.

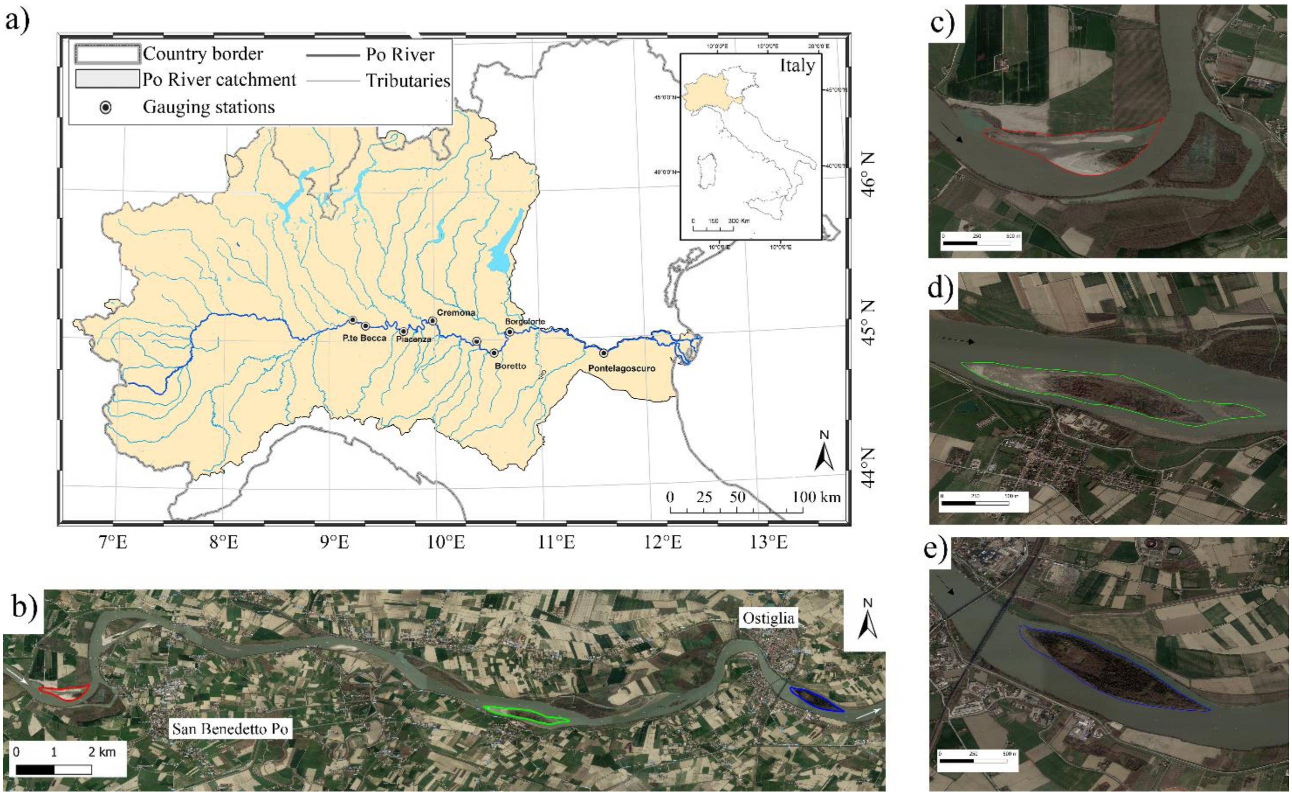

Figure 1. a) Po River basin and b) the studied areas: curve (red), central bar (green) and island (blue). Details of the area based on a Google Earth image of February 2019: c) curve, d) central bar and e) Boschina Island.

The vegetation encroachment was observed over three patterns downstream of Borgoforte: a curve, a central bar and an island (Figure 1b), characterized by a different vegetation cover in 2013. The vegetation over the curve (red area, Figure 1c) was practically absent, and the creation of a sand deposit in the inner bank moved the main channel towards the outer one. The central bar (green area, Figure 1d) is growing also because of the stabilizing effect of the vegetation. In this zone, during low flow conditions the secondary channel on the right results dry, but floods can reactivate it. The last studied part (blue area, Figure 1e) is the Boschina Island, close to the city of Ostiglia. Downstream of a railway bridge, the area is covered by permanent vegetation, mostly composed of bushes close to the river and trees in the inner part.

Evaluating such different conditions providing us with additional information about the effects of the local hydrological variations on the various vegetation stages, and consequently on the local river habitat status (Nones, 2019).

3 MATERIALS AND METHODS

3.1 Normalized Difference Vegetation Index

Satellite Remote Sensing (SRS) allows for the calculation of NDVI globally at a range of temporal intervals and spatial resolutions dependent on sensor characteristics and the satellite orbit (Robinson et al., 2017). The Landsat Mission, started in 1972, is the only uninterrupted long-term high-resolution remote sensing dataset that can provide a continuous historic NDVI record globally. Moreover, thanks to the improvements of the most recent sensors (5 ETM, 7 ETM+, 8 OLI), these 30-m resolution images are ideally suited for evaluating time-series information at the local and regional scale.

In the present application, the Landsat 8 Collection 1 Tier 1 composite is made from Tier 1 orthorectified scenes, using the computed top-of-atmosphere (TOA) reflectance (Chander et al., 2009). Landsat Tiers are the inventory structure for Landsat Collection 1 Level-1 data products and are based on data quality and level of processing. The scenes with the highest available data quality are placed into Tier 1, and include Level-1 Precision Terrain processed data that have well-characterized radiometry and are inter-calibrated across the different Landsat sensors. All Tier 1 Landsat data can be considered radiometrically calibrated and geolocated consistently (root mean square error <12 m) across the full collection for all the sensors.

The NDVI composites used in GGE are created from all the scenes in each 32-day period beginning from the first day of the year and continuing to the 352nd day of the year. The last composite of the year, beginning on day 353, will overlap the first composite of the following year by 20 days. All the images from each 32-day period are included in the composite, with the most recent pixel as the composite value.

The NDVI is generated from the Near-IR (NIR) and Red bands of each scene (eq. 1), corresponding to the band 5 and 4, respectively, and ranges from -1.0 to 1.0.

$$NDVI = \frac{NIR-Red}{NIR+Red} = \frac{band\ 5 - band\ 4}{band\ 5 + band\ 4} \qquad [1]$$

Negative values indicate the absence of vegetation (i.e., water and bare soil), while positive values denote the presence of plants. The NDVI is an indication of the vegetation density: the higher this metric, the higher the vegetation density and its maturity.

3.2 Google Earth Engine

Google Earth Engine (earthengine.google.com) is a cloud-based platform that can be used to process very large geospatial datasets, thanks to an Internet-accessible application programming interface (API) and an associated web-based interactive development environment (IDE). The platform is optimized for parallel processing to reduce computing time. The data catalogue houses a large repository, continuously updated, of publicly available geospatial datasets, including observations from several satellites and aerial imaging systems in both optical and non-optical wavelengths, comprising many environmental variables, weather and climate forecasts. The data are preprocessed to a ready-to-use but information-preserving form (Yu and Gong, 2013; Gorelick et al., 2017).

Among the plurality of datasets freely available in GEE, for this application, the Landsat8 NDVI32days images were investigated. By means of ad-hoc scripts developed accordingly to the Earth Engine Data Catalogue (developers.google.com/earth-engine/datasets/catalog/LANDSAT_LC08_C01_T1_32DAY_ NDVI), the images were monthly averaged, discarding the ones highly affected by clouds, and adjusted for focusing only on the studied regions (Figure 1b). Afterwards, the statistics of each zone were automatically extracted by using a GIS environment.

4 RESULTS AND DISCUSSION

Aiming to capture the whole vegetation season of vegetation typically observed along this Mediterranean watercourse, the analysis considered the Landsat8 images acquired from April to October (Gumiero et al., 2015). Discarded the images affected by excessive cloud cover (I.e., >20%) for avoiding bias due to clouds, the rest was averaged for obtaining one image each month for the period 2013-2017 (Table 1).

Table 1. Available Landsat8 images.

	2013	2014	2015	2016	2017
APRIL		X	X	X	
MAY		X	X		X
JUNE	X	X		X	X
JULY	X		X	X	X
AUGUST		X	X	X	
SEPTEMBER	X	X			X
OCTOBER		X	X	X	X

As visible from Figure 2, during the observed period, the mean NDVI slightly increased in all the three zones, even if the data are highly dispersed. This increment means a plausible encroachment of the vegetation, given that the local hydrology did not present significant changes that can affect the estimate.

The higher increment is observable for the bar (green squares), where the plants encountered a more suitable habitat for growing during the whole year. A similar behaviour is observable in the case of the Boschina Island (blue dots), which presents a sandbar in the upstream part of the island (Nones et al., 2018). The lower NDVI increase is measured along the curve (red diamonds), where the river results more active, therefore preventing a fast vegetation encroachment.

As for the data dispersion, the ones related to the evolving patterns observed in correspondence of the bar and the curve have a similar coefficient of determination (R^2=0.25 for the bar, R2=0.28 for the curve), while the more stable island has R^2=0.07. This can be correlated to the vegetation characteristics: the more the plants are established, the less the NDVI is a good metric in estimating the evolutive trend.

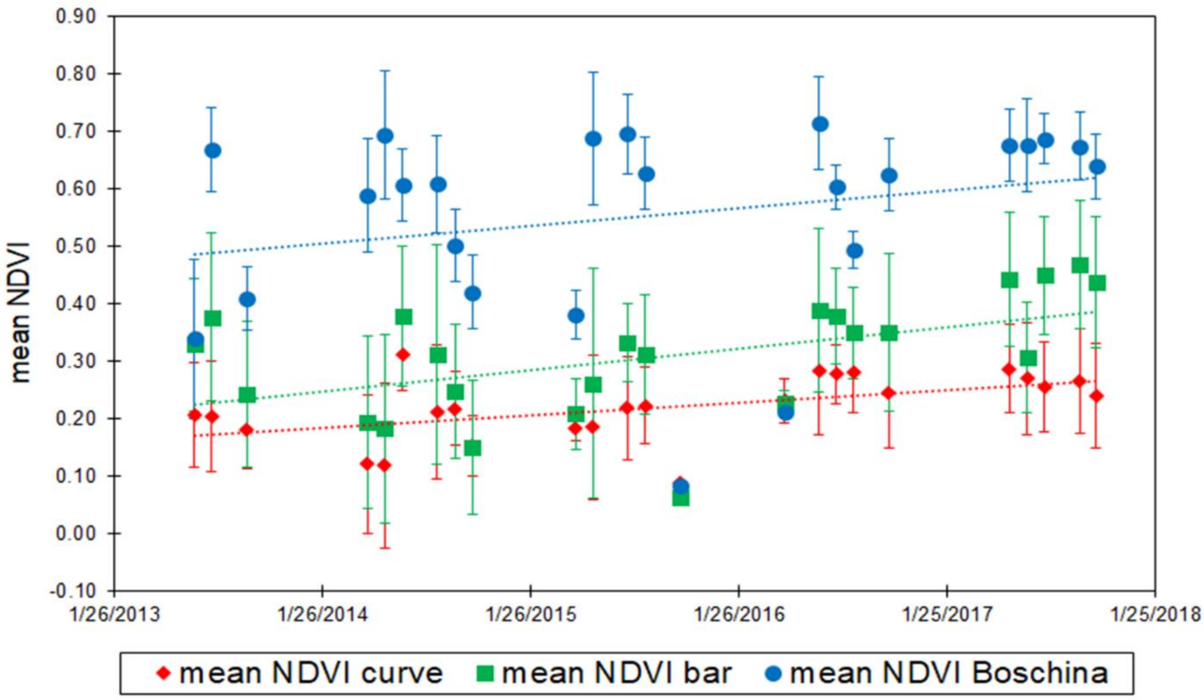

Figure 2. The trend of the mean NDVI for the three zones (curve in red, bar in green, island in blue), during the period 2013-2017.

Aside from analyzing the absolute trend of the mean NDVI, it is interesting to evaluate it as a response to the local hydrological changes (Figure 3).

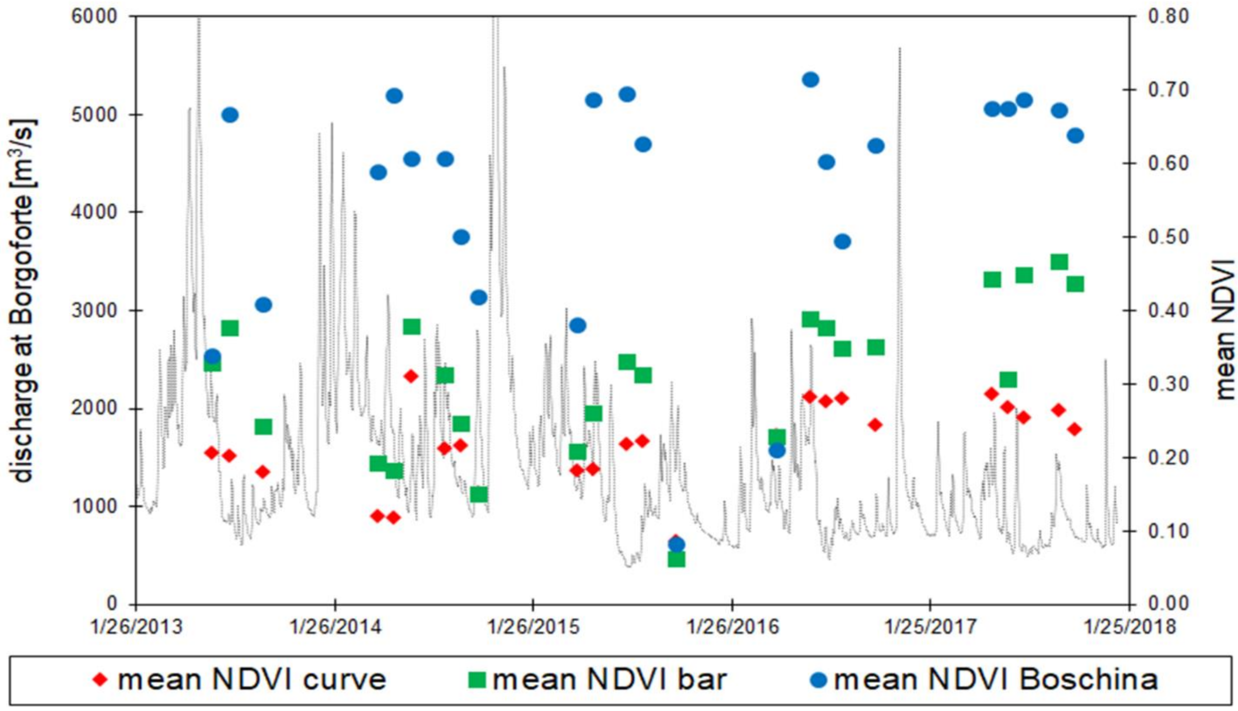

Figure 3. Comparison of the mean NDVI for the three areas (curve in red, bar in green, island in blue) with the measured discharge (black dotted line) at the upstream gauging station of Borgoforte (Mn), during the period 2013-2017.

If compared with the water discharges measured at the daily scale just upstream of the studied zones, one can observe that, even if the winter floods are necessary to re-establish the water table level, their recent reduction both in terms of magnitude and duration can only slightly contribute to the vegetation growth.

On the other part, the prolonged drought observed during the 2015-2016 period, characterized by dry summers and very low winter flooding events, stressed the vegetation, reducing the duration of the growing season. As visible, indeed, the values measured in October 2015 and April 2016 were very low if compared with the usual values measured in those months. However, once adapted to more constant, even if lower, flow conditions, the vegetation is able to re-establish itself in a proper manner, colonizing the sand deposits during the summer and fixing the soil, preventing the possible river wandering in the case of higher flow conditions.

5 CONCLUSIONS

The use of the free tool service Google Earth Engine permitted an estimate of the vegetation changes in different zones of the Po River, in Italy, analyzing the variation of the NDVI during the period 2013-2017. The study points out the existing weak correlation of such changes with the local hydrology, even at the short-time scale of observation.

The preliminary analysis reported here highlighted that, on the one part, a prolonged and significant drought can negatively affect the fluvial vegetation, potentially reducing its growing season and the opportunity to colonize new spaces. On the other part, the reduction of the flow discharge variability and especially the decrease of extreme events can provide good conditions for the vegetation encroachment, but only in the case of a rather constant flow around the long-term mean values. Indeed, in these conditions, the new plants are not disturbed by flooding events or strong droughts and have time to stably colonize the inner parts of the curve and the sandbars, changing their patterns towards vegetated islands. Once established, the plants can then continue to freely grow over such islands

Because of the short temporal horizon studied the conclusions derived here should be corroborated by future research, observing the river behaviour for longer periods and accounting for analyses at the reach scale, with the final aim to provide an estimate of the future bio-morphodynamics trend of the Po River as a response to human- and naturally-driven changes of the hydrology.

From this application, one can notice that the use of remote sensing imagery can be helpful in addressing fluvial hydro-morphological and vegetational changes at the reach scale, suggesting future trends on the basis of past observation, which can be eventually modelled with appropriate numerical codes.

ACKNOWLEDGEMENTS

The work done by Michael Nones was supported within statutory activities No. 3841/E-41/S/2019 of the Ministry of Science and Higher Education of Poland.

REFERENCES

Bechter, T., Baumann, K., Birk, S., Bolik, F., Graf, W., & Pletterbauer, F. (2018). LaRiMo-A simple and efficient GIS-based approach for large-scale morphological assessment of large European rivers. *Science of the Total Environment*, 628, 1191-1199.

Bizzi, S., Demarchi, L., Grabowski, R.C., Weissteiner, C. J., & Van de Bund, W. (2016). The use of remote sensing to characterise hydromorphological properties of European rivers. *Aquatic Sciences*, 78(1), 57-70.

Bollati, I.M., Pellegrini, L., Rinaldi, M., Duci, G., & Pelfini, M. (2014). Reach-scale morphological adjustments and stages of channel evolution: the case of the Trebbia River (northern Italy). *Geomorphology*, 221, 176-186.

Carrasco, L., O'Neil, A.W., Morton, R.D., Rowland, C.S. (2019). Evaluating Combinations of Temporally Aggregated Sentinel-1, Sentinel-2 and Landsat 8 for Land Cover Mapping with Google Earth Engine. *Remote Sensing*, 11, 288.

Castiglioni, G.B., Biancotti, A., Bondesan, M., Cortemiglia, G.C., Elmi, C., Favero, V., Gasperi, G., Marchetti, G., Orombelli, G., Pellegrini, G.B., & Tellini, C. (1999). Geomorphological map of the Po Plain, Italy, at a scale of 1: 250 000. *Earth Surface Processes and Landforms*, 24(12), 1115–1120.

Chander, G., Markham, B. L., & Helder, D. L. (2009). Summary of current radiometric calibration coefficients for Landsat MSS, TM, ETM+, and EO-1 ALI sensors. *Remote Sensing of Environment*, 113(5), 893-903.

Choi, S.U., Yoon, B., & Woo, H. (2005). Effects of dam-induced flow regime change on downstream river morphology and vegetation cover in the Hwang River, Korea. *River Research and Applications*, 21(2-3), 315-325.

Chu, H., Venevsky, S., Wu, C., & Wang, M. (2019). NDVI-based vegetation dynamics and its response to climate changes at Amur-Heilongjiang River Basin from 1982 to 2015. *Science of the Total Environment*, 650, 2051-2062.

Coltin, B., McMichael, S., Smith, T., & Fong, T. (2016). Automatic boosted flood mapping from satellite data. *International Journal of Remote Sensing*, 37(5), 993-1015.

de Jalón, D.G., Bussettini, M., Rinaldi, M., Grant, G., Friberg, N., Cowx, I.G., Magdaleno, F., & Buijse, T. (2017). Linking environmental flows to sediment dynamics. *Water Policy*, 19(2), 358-375.

Diehl, R.M., Wilcox, A.C., Stella, J.C., Kui, L., Sklar, L.S., & Lightbody, A. (2017). Fluvial sediment supply and pioneer woody seedlings as a control on bar-surface topography. *Earth Surface Processes and Landforms*, 42(5), 724-734.

Domeneghetti, A., Carisi, F., Castellarin, A., & Brath, A. (2015). Evolution of flood risk over large areas: Quantitative assessment for the Po River. *Journal of Hydrology*, 527, 809-823.

Dong, J., Xiao, X., Menarguez, M.A., Zhang, G., Qin, Y., Thau, D., Chandrashekhar, C., & Moore III, B. (2016). Mapping paddy rice planting area in northeastern Asia with Landsat 8 images, phenology-based algorithm and Google Earth Engine. *Remote Sensing of Environment*, 185, 142-154.

Edmonds, D.A., Hajek, E.A., Downton, N., & Bryk, A. B. (2016). Avulsion flow-path selection on rivers in foreland basins. *Geology*, 44(9), 695-698.

Eke, E., Parker, G., & Shimizu, Y. (2014). Numerical modeling of erosional and depositional bank processes in migrating river bends with self-formed width: Morphodynamics of bar push and bank pull. *Journal of Geophysical Research: Earth Surface*, 119(7), 1455-1483.

Fergus, T. (1997). Geomorphological response of a river regulated for hydropower: River Fortun, Norway. *Regulated Rivers: Research & Management*, 13(5), 449-461.

Gorelick, N., Hancher, M., Dixon, M., Ilyushchenko, S., Thau, D., & Moore, R. (2017). Google Earth Engine: Planetary-scale geospatial analysis for everyone. *Remote Sensing of Environment*, 202, 18-27.

Guerrero, M., Di Federico, V., & Lamberti, A. (2013). Calibration of a 2-D morphodynamic model using water-sediment flux maps derived from an ADCP recording. *Journal of Hydroinformatics*, 15(3), 813-828.

Gumiero, B., Rinaldi, M., Belletti, B., Lenzi, D., & Puppi, G. (2015). Riparian vegetation as indicator of channel adjustments and environmental conditions: the case of the Panaro River (Northern Italy). *Aquatic Sciences*, 77(4), 563-582.

Hansen, M.C., Potapov, P.V., Moore, R., Hancher, M., Turubanova, S.A.A., Tyukavina, A., Thau, D., Stehman, S.V., Goetz, S.J., Loveland, T.R., Kommareddy, A., Egorov, A., Chini, L., Justice, C.O., & Townshend, J.R.G. (2013). High-resolution global maps of 21st-century forest cover change. *Science*, 342(6160), 850-853.

Huete, A., 2016. Vegetation's responses to climate variability. *Nature*, 531, 181–182.

Isikdogan, F., Bovik, A., & Passalacqua, P. (2017). RivaMap: An automated river analysis and mapping engine. *Remote Sensing of Environment*, 202, 88-97.

Lamberti, A., & Schippa, L. (1994). Studio dell'abbassamento del fiume Po: Previsioni trentennali di abbassamento a Cremona. *Supplemento a Navigazione Interna, rassegna trimestrale di studi e informazioni*, 3/4. Azienda Regionale per i porti di Cremona e Mantova, Cremona, Italy. in Italian

Lanzoni, S., Luchi, R., Bolla Pittaluga, M. (2015). Modeling the morphodynamic equilibrium of an intermediate reach of the Po River (Italy). *Advances in Water Resources*, 81, 92-102.

Lobell, D.B., Thau, D., Seifert, C., Engle, E., & Little, B. (2015). A scalable satellite-based crop yield mapper. *Remote Sensing of Environment*, 164, 324-333.

Marchetti, M. (2002). Environmental changes in the central Po Plain (northern Italy) due to fluvial modifications and anthropogenic activities. *Geomorphology*, 44(3-4), 361–73.

Markert, K.N., Schmidt, C.M., Griffin, R.E., Flores, A.I., Poortinga, A., Saah, D.S., Muench, R.E., Clinton, N.E., Chishtie, F., Kityuttachai, K., Someth, P., Anderson, E.R., Aekakkararungroj, A., & Ganz, D.J. (2018). Historical and operational monitoring of surface sediments in the Lower Mekong basin using Landsat and Google Earth Engine cloud computing. *Remote Sensing*, 10(6), 909.

Maselli, V., Pellegrini, C., Del Bianco, F., Mercorella, A., Nones, M., Crose, L., Guerrero, M., & Nittrouer, J.A. (2018). River Morphodynamic Evolution Under Dam-Induced Backwater: An Example from the Po River (Italy). *Journal of Sedimentary Research*, 88(10), 1190-1204.

Monegaglia, F., Zolezzi, G., Güneralp, I., Henshaw, A.J., & Tubino, M. (2018). Automated extraction of meandering river morphodynamics from multitemporal remotely sensed data. *Environmental Modelling & Software*, 105, 171-186.

Montanari, A. (2012). Hydrology of the Po River: Looking for changing patterns in river discharge. *Hydrology and Earth System Sciences*, 16(10), 3739-3747

Musolino, D., de Carli, A., & Massarutto, A. (2017). Evaluation of the socioeconomic impacts of the drought events: the case of the Po River basin. *European Countryside*, 9(1), 163-176.

Nones, M., Ronco, P., & Di Silvio, G. (2013). Modelling the impact of large impoundments on the Lower Zambezi River. *Int. Journal of River Basin Management*, 11(2), 221-236.

Nones, M., Archetti, R., & Guerrero, M. (2018). Time-Lapse Photography of the Edge-of-Water Line Displacements of a Sandbar as a Proxy of Riverine Morphodynamics. *Water*, 10, 617.

Nones, M. (2019) Numerical Modelling as a Support Tool for River Habitat Studies: An Italian Case Study. *Water*, 11, 482.

Patel, N.N., Angiuli, E., Gamba, P., Gaughan, A., Lisini, G., Stevens, F.R., Tatem, A.J., & Trianni, G. (2015). Multitemporal settlement and population mapping from Landsat using Google Earth Engine. *International Journal of Applied Earth Observation and Geoinformation*, 35, 199-208.

Pekel, J.F., Cottam, A., Gorelick, N., & Belward, A. S. (2016). High-resolution mapping of global surface water and its long-term changes. *Nature*, 540(7633), 418.

Robinson, N.P., Allred, B.W., Jones, M.O., Moreno, A., Kimball, J.S., Naugle, D.E., Erickson, T.A., Richardson, A.D. (2017). A Dynamic Landsat Derived Normalized Difference Vegetation Index (NDVI) Product for the Conterminous United States. *Remote Sensing*, 9, 863.

Rouse Jr.J., Haas, R.H., Schell, J.A., & Deering, D.W. (1974). Monitoring vegetation systems in the Great Plains with ERTS. *Proceedings of the Third Earth Resources Technology Satellite-1 Symposium*, Washington, DC, USA.

Shelestov, A., Lavreniuk, M., Kussul, N., Novikov, A., & Skakun, S. (2017). Exploring Google earth engine platform for Big Data Processing: Classification of multi-temporal satellite imagery for crop mapping. *Frontiers in Earth Science*, 5, 17.

Soulard, C.E., Albano, C.M., Villarreal, M.L., & Walker, J. J. (2016). Continuous 1985–2012 Landsat monitoring to assess fire effects on meadows in Yosemite National Park, California. *Remote Sensing*, 8(5), 371.

Sturrock, H.J., Cohen, J.M., Keil, P., Tatem, A.J., Le Menach, A., Ntshalintshali, N.E., Hsiang, M.S., & Gosling, R.D. (2014). Fine-scale malaria risk mapping from routine aggregated case data. *Malaria Journal*, 13(1), 421.

Tsai, Y.H., Stow, D., Chen, H.L., Lewison, R., An, L., & Shi, L. (2018). Mapping Vegetation and Land Use Types in Fanjingshan National Nature Reserve Using Google Earth Engine. *Remote Sensing*, 10(6), 927.

Tucker, C.J., Miller, L.D., & Pearson, R.L. (1973). Measurement of the combined effect of green biomass, chlorophyll, and leaf water on canopy spectroreflectance of the shortgrass prairie. *Remote Sensing of Earth Resources*, 2.

Yang, J., Gong, P., Fu, R., Zhang, M., Chen, J., Liang, S., Xu, B., Shi, J. & Dickinson, R. (2013). The role of satellite remote sensing in climate change studies. *Nature Climate Change*, 3, 875-883.

Yu, L., & Gong, P. (2012). Google Earth as a virtual globe tool for Earth science applications at the global scale: progress and perspectives. *International Journal of Remote Sensing*, 33(12), 3966-3986.

Zanchettin, D., Traverso, P., & Tomasino, M. (2008). Po River discharges: a preliminary analysis of a 200-year time series. *Climatic Change*, 89(3-4), 411-433.

Zhang, Q., Li, B., Thau, D., & Moore, R. (2015). Building a better urban picture: Combining day and night remote sensing imagery. *Remote Sensing*, 7(9), 11887-11913.